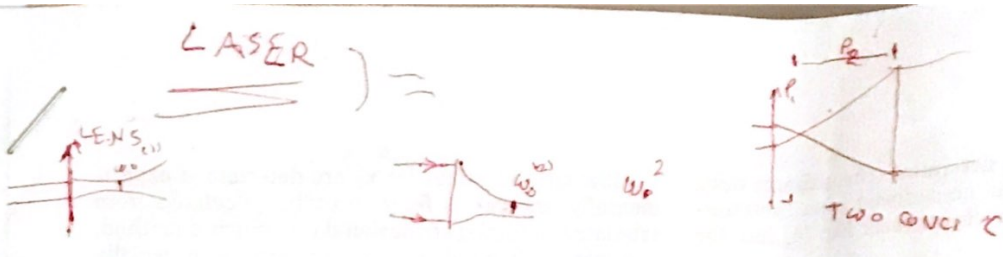

Measurement of a Gaussian laser beam diameter through the direct inversion of knife-edge data

John M. Khosrofian and Bruce A. Garetz

An inversion algorithm, involving a linear least-squares method, is developed to analyze the intensity data obtained by application of the traveling knife-edge method. Through use of simulated intensity data, diameters can be measured to an accuracy of 0.05%. The method also yields good results when it is applied to He–Ne laser beam data.

I. Introduction

The application of lasers to investigation of many chemical and biophysical phenomena requires knowledge of the diameter of the incident beam or the waist diameter of a focused beam. Although techniques such as ray tracing,[1] multiphoton ionization yields,[2] and fluorescence correlation spectroscopy[3] predict accurate results, such methods are either too complicated for most general applications or they rely on specific experimental procedures not easily adaptable to other experiments. Other more direct methods for determination of beam diameters include correlation of the square of the diameter of a spot burned by the laser beam with the logarithm of the normalized power absorbed from the beam by the material that incurs the damage.[4] In addition, the intensity profile of the laser beam can be probed directly either by a photoelectric or pyroelectric detector array.[5]

Another class of method involves gradual eclipsing of the laser beam by a sharp knife-edge. As the knife-edge intersects the beam in a direction perpendicular to the propagation axis of the beam, a photodetector measures the intensity of the unmasked portion of the beam. If the spatial profile of the laser beam is described by a Gaussian line shape, the signal measured by the detector is represented by an integrated Gaussian function. In principle, the beam diameter can be determined from such photodetector data. One approach involves electronic[6] or numerical[7] differentiation of the experimental data, thus reconstructing the original Gaussian profile.

We present here an alternative method for analyzing knife-edge data. In the course of this paper, we will describe the mathematical procedure by which knife-edge data are inverted to yield accurate beam diameter values as well as presenting an experimental demonstration of the method using a He–Ne laser.

II. Theory

The cross-sectional spatial profile of a Gaussian laser beam propagating in the z direction is given by the function

$$G(x,y) = I_0 \exp[-\beta^2 r^2(x,y)], \tag{1}$$

in which $r(x,y) = [(x-x_0)^2 + (y-y_0)^2]^{1/2}$, where x_0,y_0 define the center of the beam profile. I_0 is the maximum value of $G(x,y)$ measured at the center, and β^{-1} is the radius at which $G(x,y)$ falls to $1/e$ times its maximum value I_0 (~37%).

Although the distribution given in Eq. (1) is radially symmetric, the present procedure involves a linear 1-D translation of the knife-edge. If the x axis is chosen as the translation axis, the response of the photodetector to the transmitted portion of the beam is given by

$$R(x_b) = \int_{-\infty}^{\infty} \int_{-\infty}^{x_b} G(x,y)\,dx\,dy, \tag{2}$$

where x_b is the x coordinate of the knife-edge when the measurement is made. Evaluation of Eq. (2) yields

$$R(x_b) = I_0(\pi/\beta^2)^{1/2} \int_{-\infty}^{x_b} \exp[-\beta^2(x-x_0)^2]\,dx. \tag{3}$$

This response can be normalized to the total integrated signal of the full totally unmasked beam ($x_b \to \infty$) by

$$\tilde{R}(x_b) = R(x_b)/R(\infty) = \beta\pi^{-1/2} \int_{-\infty}^{x_b} \exp[-\beta^2(x-x_0)^2]\,dx, \tag{4}$$

where $\tilde{R}$ represents the normalized response function.

The authors are with Polytechnic Institute of New York, Chemistry Department, Brooklyn, New York 11201.

Received 1 July 1983.
0003-6935/83/213406-05$01.00/0.

In principle, β, which determines the ultimate value for the beam radius, can be deduced from the transformation condition which converts Eq. (4) into the normal distribution:

$$N(z) = (2\pi)^{1/2} \int_{-\infty}^{z} \exp(-n^2/2)dn. \tag{5}$$

The salient difference between $\bar{R}(x)$ and $N(z)$ is found in the arguments of the exponents in the integrands. The two arguments can be made equal if the condition

$$n^2/2 = \beta^2(x - x_0)^2 \tag{6}$$

is imposed. Solving Eq. (6) for n yield

$$n = \sqrt{2}\beta x - \sqrt{2}\beta x_0 \tag{7}$$

or in differential form

$$dn = \sqrt{2}\beta dx. \tag{8}$$

In addition, Eq. (7) provides a simple linear function which can be used to determine β, if the correspondence between the experimentally determined translation points x and the equivalent points n of the normal distribution is known. To separate β from x_0, Eq. (7) can be rewritten as

$$x = \frac{n}{\sqrt{2}\beta} + x_0, \tag{9}$$

or, evaluated for a particular measurement,

$$x_b = \frac{z}{\sqrt{2}\beta} + x_0. \tag{10}$$

Since Eq. (9) is a linear equation with two unknown quantities β^{-1} and x_0, only two pairs of data points (z,x_b) are necessary to uniquely determine the two unknowns.[8,9] For example, one could measure the x_b values at which the beam intensity falls to 10 and 90% of the full value. From a normal distribution table, the values of z at which the normal distribution $N(z)$ equals 0.10 and 0.90 are found to be ± 1.28. This information provides two simultaneous equations:

$$x_{10} = \frac{1.28}{\sqrt{2}\beta} + x_0; \tag{11a}$$

$$x_{90} = -\frac{1.28}{\sqrt{2}\beta} + x_0, \tag{11b}$$

which when solved yields

$$x_0 = (x_{10} + x_{90})/2 \tag{12a}$$

$$\beta^{-1} = 0.552(x_{10} - x_{90}). \tag{12b}$$

However, such an approach to the problem has disadvantages. Each experimentally measured translation point contains an inherent random error which is propagated to β through Eq. (10). Furthermore, the method provides no indication of how closely the spatial intensity profile of the laser beam resembles a Gaussian line shape. The best approach is application of the method of least squares to Eq. (10) for a large number of data pairs. After β and x_0 have been determined, Eq. (10) can be used to generate either the best fit profile or the degree of correlation of the experimental data with the theory.

Although the values for x_b are determined experimentally, the values for z must be calculated from tabulated normal distribution data. Such a method, however, is often tedious and cumbersome, especially for a large number of data points. A better procedure is use of an analytic approximation for the normal distribution to generate the values of z. Such an approach also obviates the necessity of either storing or reentering the tabulated normal distribution into a limited memory. As an initial approximation, the function

$$f(z) = \frac{1}{1 + \exp(-z)} \tag{13}$$

is a good representation for the extrema of the normal distribution; as z approaches + or − infinity, $f(z)$ converges to unity and zero, respectively, and $f(z)$ assumes the value 0.5 for $z = 0$. However, a better representation for a wider range of values can be obtained by replacement of z by a polynomial expansion in z:

$$P(z) = \sum_{i=0}^{m} a_i z^i \tag{14}$$

as a result of Eq. (12), Eq. (13) can be modified:

$$f(z) = \frac{1}{1 + \exp[P(z)]}. \tag{15}$$

The values for m, the order of the polynomial, and the coefficients $\{a_i\}$ can be determined by application of the method of least squares to the logarithmic transform of Eq. (15):

$$P(z) = \log[f^{-1}(z) - 1] \tag{16}$$

and the use of the data from the tabulated normal distribution function.[10] The least-squares analysis generates a third-order polynomial with coefficients

$$\begin{aligned} a_0 &= -6.71387 \times 10^{-3}, \\ a_1 &= -1.55115, \\ a_2 &= -5.13306 \times 10^{-2}, \\ a_3 &= -5.49164 \times 10^{-2}, \end{aligned} \tag{17}$$

which correspond to a maximum correlation of 0.999891. The normal distribution data consist of every tenth listing in Table V of Ref. 10

After the values of the polynomial coefficients have been established, $f(z)$ can be used to determine z from $\bar{R}(x_b)$, the experimentally measured normalized response function, by the method of successive approximations; the value of z is changed by successively smaller increments, and $f(z)$ is compared with $\bar{R}(x_b)$ until

$$\bar{R}(x_b) = f(z) \tag{18}$$

to the desired degree of accuracy.

III. Experimental Procedure

The knife-edge translator which was used to probe the beam intensity profile is illustrated in Fig. 1. It consists of a micrometer-driven translation stage, to which is secured a single-edge razor blade. Beam diameter measurements were performed on a cw He–Ne

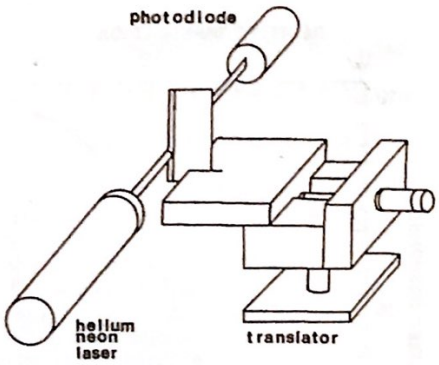

Fig. 1. Schematic diagram of the experimental configuration.

laser with an output power of 2 mW at 632.8 nm. The knife-edge was advanced through the beam in equal steps of 25.4 μm. The integrated intensity of the uneclipsed portion of the beam was measured by a PIN diode operating in the photovoltaic mode. The voltage signal was measured on a Tektronix 7704 oscilloscope.

IV. Discussion

A. Computer Program

The computer program which analyzes the experimental data was written in BASIC language for a Commodore 8K PET microcomputer. The program is easily modified for use with other comparable computers.

The experimental response data are entered serially into the computer memory. These data are corrected for a predetermined background and normalized to the maximum response signal, which corresponds to the signal from a totally uneclipsed beam.

A translation axis is set up internally in the computer so that one translation unit corresponds to a single step of the micrometer head. In our experiments, a single step corresponds to a distance $\delta = 25.4$ μm of actual translation.

The normalization of the response data produces a set of normalized responses $\bar{R}(x_b)$ which range between zero and unity. To determine the value of z, the normalized translation distance corresponding to each $\bar{R}(x_b)$ as described in Eq. (18), a regression technique is used to approximate the numerical inversion of Eq. (15). The value for z is varied, initially from zero to a predetermined upper limit by increments of 0.1, until z assumes the largest value for which

$$f(z) \le \bar{R}(x_b). \tag{19}$$

The algorithm is repeated three times, beginning with the current value of z, with the value for the increment diminished by a factor of 10 for each repetition. The final value of z is expressed to four decimal places.

The procedure that has been presented is valid only for $\bar{R}(x_b) \ge 0.5$, because the parameters that define $f(z)$ have been determined from tabulated normal data with positive arguments. To extend the procedure to include negative arguments of $\bar{R}(x_b)$ and $f(z)$, the reflection symmetry of the Gaussian line shape about the origin is applied as follows:

$$\bar{R}(-x_b) = \int_{-\infty}^{-x_b} G(x)dx = \int_{x_b}^{\infty} G(x)dx$$
$$= \int_{-\infty}^{\infty} G(x)dx - \int_{-\infty}^{x_b} G(x)dx = 1 - \bar{R}(x_b). \tag{20}$$

Similarly,

$$f(-z) = 1 - f(z). \tag{21}$$

In the actual execution of the program, $\bar{R}(-x_b)$ is replaced by $-\bar{R}(x_b)$. The negative sign is used as a label to indicate that the value for z that is calculated from the absolute value of $-\bar{R}(x_b)$ should be stored in memory as $-z$.

The method of least squares is used to fit the pairs (x_b,z) to a straight line, thus determining β and x_0 in dimensionless units. The corresponding dimensioned quantities are β/δ and $x_0\delta$, where δ is the micrometer calibration factor. The program for the analysis is available upon request.

B. Analysis of Results

To establish the accuracy of the numerical procedure for determination of β, simulated profiles corresponding to particular values of β were generated from tabulated normal distribution data through use of Eq. (10). Best-fit values of β were determined using the described algorithm and were compared to the exact β values. The fits were excellent, with agreement to 0.05%.

In addition, the calculated β values were used to generate the best-fit profiles. Comparison of exact and calculated profiles is shown in Figs. 2 and 3 for two different values of β.

The results from analysis of experimental data for a He–Ne laser are presented in Fig. 4, which depicts a typical profile from a series of eleven measurements. The beam diameter d with respect to the $1/e^2$ points of the Gaussian line shape is related to β through the expression

$$d = 2\sqrt{2}\beta^{-1}. \tag{22}$$

The values of the beam diameter based on eleven independent measurements were 0.67 ± 0.02 mm. The variations among the five measurements are probably due to a variety of sources, including some instability in the mounting of the translator and to fluctuations in the laser beam intensity. The former problem can be alleviated through a more secure mounting of the translator. The latter could be surmounted by splitting off a fraction of the laser beam and normalizing all measurements with respect to this reference intensity.

The sensitivity of the translation can be increased by rotating the knife-edge in its mount by an angle θ, measured from the initial vertical position of the knife-edge. As a result, the direction of translation is also rotated by the angle θ, in the plane perpendicular to the direction of propagation of the laser beam. If the knife-edge passes through a distance δ before the rotation, the corresponding translation distance for the rotated knife-edge is the projection of δ along the new

direction of translation or $\delta \cos\theta$. Such a procedure eliminates the need for a micrometer drive with a finer pitch when higher sensitivity is required.

V. Conclusions

The results demonstrate that the knife-edge method used in conjunction with the described algorithm for the analysis of the detector data provides a relatively simple procedure for accurately measuring the diameter of a Gaussian laser beam. In particular, the algorithm (Fig. 5) consists of a straightforward numerical technique for direct analysis of the experimental data rather than first reconstructing a Gaussian distribution.

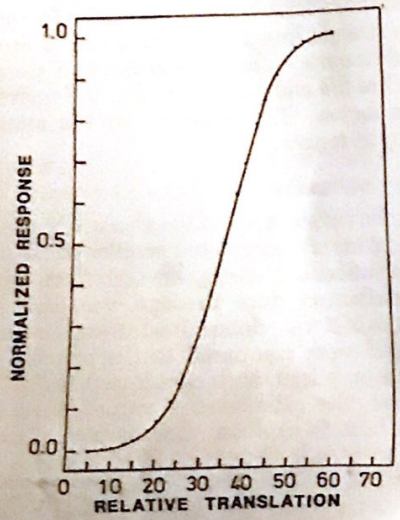

Fig. 2. Integrated Gaussian profile for $\beta = (\sqrt{2})^{-1}$. Solid dots indicate experimental data points, and the solid line represents the best-fit profile.

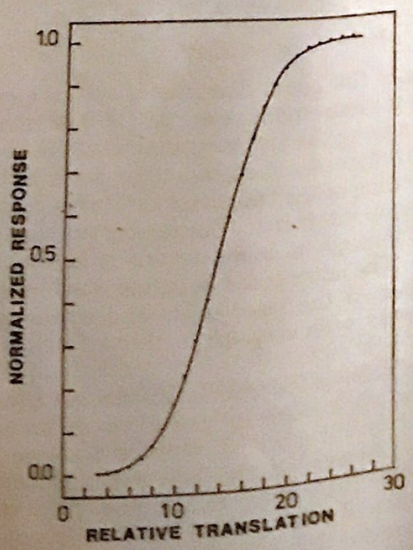

Fig. 3. Integrated Gaussian profile for $\beta = 0.177$. Solid dots indicate experimental data points, and solid line represents the best-fit profile.

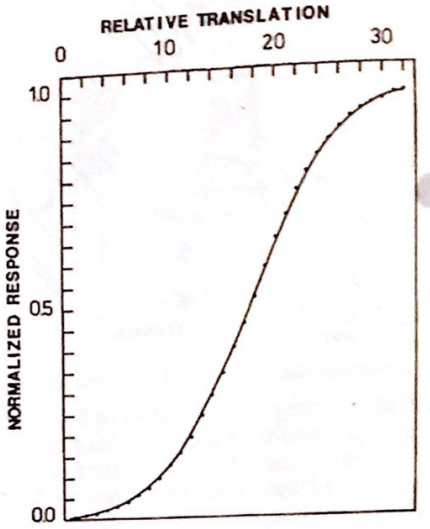

Fig. 4. Integrated Gaussian profile for the He–Ne laser beam. A single translation step corresponds to 25.4 μm. Solid dots indicate experimental data points, and the solid line represents the best-fit profile.

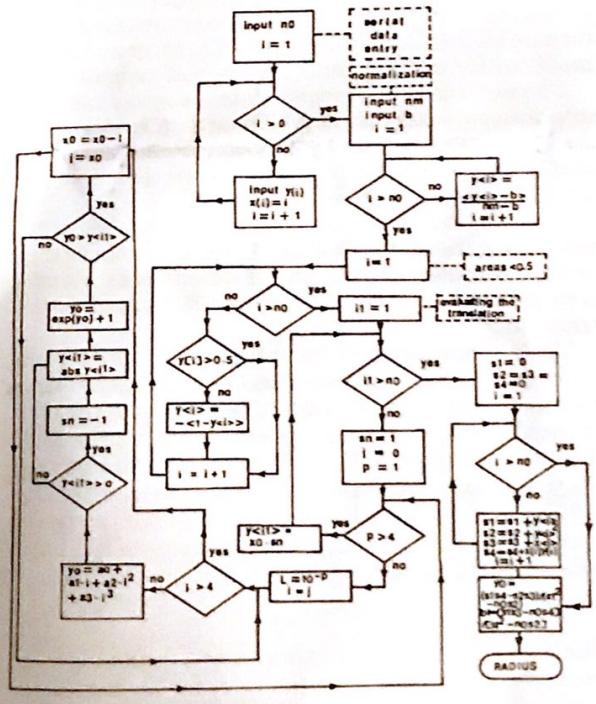

Fig. 5. Schematic flow chart for the computer algorithm.

Acknowledgment is made to the National Science Foundation (grant ECS-7908109), the Research Corp., and the Petroleum Research Fund, administered by the American Chemical Society, for support of this research.

References

1. G. Rinker and G. Bohannon, IEEE Trans. Plasma Sci. PS-8, 55 (1980).
2. B. H. A. Granneman and M. J. van der Wiel, Rev. Sci. Instrum. 46, 332 (1975).
3. S. M. Sorscher and M. P. Klein, Rev. Sci. Instrum. 51, 98 (1980).
4. Y. C. Kiang and R. W. Lang, Appl. Opt. 22, 1296 (1983).
5. J. G. Edwards, H. R. Gallantree, and R. M. Quilliam, J. Phys. E 10, 699 (1977).
6. J. A. Arnaud, W. M. Hubbard, G. D. Mandeville, B. de la Claviere, E. A. Franke, and J. M. Franke, Appl. Opt. 10, 2775 (1971).
7. M. Mauck, Appl. Opt. 18, 599 (1979).
8. Y. Suzaki and A. Tachibana, Appl. Opt. 14, 2809 (1975).
9. *Laser Handbook*, (Metrologic Instruments, Bellmar, N.J. 1979), p. 28.
10. H. D. Brunk, *An Introduction to Mathematical Statistics* (Blaisdell, Waltham, Mass., 1965), p. 389.

OTA REPORT BRIEF

For many years to come, energy need not constrain economic growth in the United States. OTA projects that over the next two decades, investments in new manufacturing processes, a shift to less energy-intensive products, and technical innovation will lead to substantially increased energy efficiency. At the same time, these improvements will increase industrial profitability and competitiveness. As a result, OTA projects **that the rate of industrial production can grow considerably faster than the rate of energy use needed for that production.**

Corporate investment decisionmaking appears to recognize this link between productivity and energy efficiency. All corporate projects are evaluated in terms of product demand, competition, cost of capital, cost of labor, energy and materials, and Government policy. Energy-related projects are only part of an overall strategy to improve profitability and enhance a corporation's competitive position. OTA has found that corporate capital projects directed solely at improving energy efficiency are not given special status, although energy cost is an important consideration in investment decisions.

OTA examined the four most energy-intensive industries in the U.S. manufacturing sector: paper, petroleum refining, chemicals, and steel. Historical energy use was analyzed, new technologies identified that could improve energy efficiency, and future energy demand projected. **In the paper industry, energy use has risen slightly since 1972, but the industry is now more energy self-sufficient.** In 1981, the pulp and paper industry generated half of its energy needs from wood residues.

From now through 2000, **projections for the petroleum refining industry show a decline in product output, but continued improvement in energy efficiency, although only slightly.** Efficiency gains will be offset by a shift to high-sulfur, heavier crude oil feedstock, and a need for additional processing of raw materials to meet market demand for high-octane, unleaded gasoline.

Projections for the chemicals industry indicate an increase in energy efficiency through a combination of technological improvements to existing process equipment, technical innovation in developing new processes, and a shift from commodity chemicals, such as chlorine, to less energy-intensive specialty chemicals, such as pharmaceuticals.

As the steel industry rebuilds to meet foreign competition, production will grow slowly, and will show a large reduction in energy intensity due to greater use of two new processes: the replacement of ingot casting by continuous casting, and the substitution of electric arc furnaces for the blast furnace/basic oxygen furnace combination of traditional steelmaking.

OTA examined four policy options for their effects on industrial energy use. Two options were directed specifically at energy conservation investments, while the remaining two were aimed at stimulating all investment.

OTA's findings suggest that **the most effective Government policies to promote the efficient use of energy are not those specifically targeted to energy use, but those that improve the economic outlook and investment climate by lowering interest rates and expanding demand for goods and services.** Specifically, OTA concludes that:

- **Reduction in capital costs** would be the most effective means of stimulating investments that increase energy efficiency. It would also enhance the effect of the recently enacted accelerated cost recovery system (ACRS).
- **ACRS depreciation** is a positive stimulus to investment, and thus to energy conservation. But, this effect is only significant when industry is profitable and growing.
- **Energy investment tax credits** at a 10-percent level have little direct influence on capital allocation decisions in large American firms, and thus have little or no effect on energy conservation. However, energy investment tax credits aimed at third-party financing of energy production, such as cogeneration of steam and electricity, would be effective.
- **A tax on premium fuels** would stimulate investment in energy-efficient processes and products but would also have negative effects. For example, a premium fuels tax would increase the chemicals industry's vulnerability to foreign competition and adversely affect product sales of the petroleum refining industry.

Copies of the full OTA report, "Industrial Energy Use," are available from the U.S. Government Printing Office. The GPO stock number is 052-003-00915-3; the price is $6.00. Copies of the report for congressional use are available by calling 4-8996. Summaries of the report are available at no charge from the Office of Technology Assessment.